A Conductance Maximum Observed in an Inward-Rectifier Potassium Channel

ZHE LU and RODERICK MACKINNON

From the Department of Neurobiology, Harvard Medical School, Boston, Massachusetts 02115

ABSTRACT One prediction of a multi-ion pore is that its conductance should reach a maximum and then begin to decrease as the concentration of permeant ion is raised equally on both sides of the membrane. A conductance maximum has been observed at the single-channel level in gramicidin and in a Ca^{2+}-activated K^+ channel at extremely high ion concentration (> 1,000 mM) (Hladky, S. B., and D. A. Haydon. 1972. *Biochimica et Biophysica Acta.* 274:294–312; Eisenmam, G., J. Sandblom, and E. Neher. 1977. *In* Metal Ligand Interaction in Organic Chemistry and Biochemistry. 1–36; Finkelstein, P., and O. S. Andersen. 1981. *Journal of Membrane Biology.* 59:155–171; Villarroel, A., O. Alvarez, and G. Eisenman. 1988. *Biophysical Journal.* 53:259*a*. [Abstr.]). In the present study we examine the conductance-concentration relationship in an inward-rectifier K^+ channel, ROMK1. Single channels, expressed in *Xenopus* oocytes, were studied using inside-out patch recording in the absence of internal Mg^{2+} to eliminate blockade of outward current. Potassium, at equal concentrations on both sides of the membrane, was varied from 10 to 1,000 mM. As K^+ was raised from 10 mM, the conductance increased steeply and reached a maximum value (39 pS) at 300 mM. The single-channel conductance then became progressively smaller as K^+ was raised beyond 300 mM. At 1000 mM K^+, the conductance was reduced to ~75% of its maximum value. The shape of the conductance-concentration curve observed in the ROMK1 channel implies that it has multiple K^+-occupied binding sites in its conduction pathway.

INTRODUCTION

A truly remarkable feature of ion conduction in K^+ channels is that the permeation pathway appears to accommodate multiple K^+ ions in a queue. Hodgkin and Keynes (1955) provided the first evidence for a multi-ion conduction pathway in voltage-dependent K^+ channels by showing that the unidirectional K^+ fluxes across the Cuttlefish giant axon membrane were coupled. They reasoned that a long pore containing several ions would cause ions moving in one direction to strongly influence those moving in the opposite direction. The degree of coupling measured in their experiments suggested that perhaps three ions can simultaneously reside in the pore of a K^+ channel.

Independent support for a multi-ion conduction mechanism has also come from studies using blocking ions that enter the pore of K^+ channels. In a high-conductance Ca^{2+}-activated K^+ channel, blockade by Na^+ was influenced by the K^+ concentration

J. GEN. PHYSIOL. © The Rockefeller University Press · 0022-1295/94/09/0477/10 $2.00
Volume 104 September 1994 477–486

on the opposite side of the membrane as if both Na^+ and K^+ could reside in the pore simultaneously (Yellen, 1984). Very often, the voltage dependence of ion blockade is anomalously high if one assumes that voltage dependence arises solely from a charged blocker moving through the transmembrane electric field (Armstrong, Swenson, and Taylor, 1982; French and Shoukimas, 1985; Cecchi, Wolff, Alvarez, and Latorre, 1987). The excess voltage dependence implies that the movement of a blocking ion may be coupled to the movement of other permeant ions also present in the pore. By studying the residence time of a blocking Ba^{2+} in a Ca^{2+}-activated K^+ channel, Neyton and Miller (1988) showed that K^+ binds at a site in the pore even when a Ba^{2+} ion is already present.

A third manifestation of multi-ion conduction in K^+ channels has been termed the anomalous mole fraction effect (Hagiwara, Miyazaki, Krasne, and Ciani, 1977; Eisenman, Latorre, and Miller, 1986; Wagoner and Oxford, 1987; Shapiro and DeCoursey, 1991; Heginbotham and MacKinnon, 1993). The anomalous mole fraction effect, a phenomenon first described in glass conductors (Eisenman, Sandblom, and Walker, 1967), refers to the peculiar behavior of conductance (or reversal potential in the case of an inward rectifier K^+ channel) in mixtures of two permeant ions. In high-conductance Ca^{2+}-activated K^+ channels as well as *Shaker* voltage-activated K^+ channels, for example, the conductance is larger in the presence of pure NH_4Cl or KCl solutions than in the presence of mixtures of the two ions (Eisenman et al., 1986; Heginbotham and MacKinnon, 1993). The favored explanation is that at least two ions can be present simultaneously within the conduction pathway, and that a higher conductance is sustained when the ions are of the same species.

A fourth expected property of a channel that allows two or more ions to coexist along the conduction pathway is inhibition of conduction when the ion concentration is raised to sufficiently high levels on both sides of the membrane (Hille and Schwarz, 1978; Kohler and Heckmann, 1979; Schumaker and MacKinnon, 1990). Experimentally, the effect should be identifiable as a descending phase of the conductance-concentration relationship at high ion concentrations. The theoretical basis has been described in detail, but the actual phenomenon is very rare in K^+ channels, having only been observed at the single-channel level in the case of a high-conductance Ca^{2+}-activated K^+ channel at concentrations of Rb^+ above 2,000 mM (Villarroel, Alvarez, and Eisenman, 1988). In squid axon delayed-rectifier K^+ channels, macroscopic currents exhibited a descending phase at concentrations above 1,000 mM (Wagoner and Oxford, 1987). However, *Shaker* K^+ channels expressed in *Xenopus* oocytes also exhibit a descending phase when macroscopic currents are examined (our unpublished results), but no descending phase is observed in single-channel conductance even at K^+ concentrations up to 2,000 mM (Heginbotham and MacKinnon, 1993). In the present study, we investigate the variation of single-channel conductance as a function of K^+ in an inward rectifier K^+ channel (ROMK1), cloned from rat kidney outer medulla (Ho, Nichols, Lederer, Lytton, Vassilev, Kanazirska, and Herbert, 1993). Surprisingly, a descending phase begins at a concentration as low as 300 mM K^+. The data can be interpreted in terms of a two-site single–vacancy conduction model (Schumaker and MacKinnon, 1990). The qualitative difference between the conductance-concentration behavior of ROMK1 and *Shaker* K^+ channels can be accounted for by a sevenfold difference in the rate constant for K^+ entry.

METHODS

Molecular Biology and Oocyte Preparation

DNA encoding the ROMK1 channel present in the p-SPORT1 plasmid (Gibco-BRL, Gaithersburg, MD) was kindly provided by Drs. Ho and Hebert (Ho et al., 1993). RNA was synthesized from NOT1 (NEB)-linearized DNA using T7 polymerase (Promega Corp., Madison, WI). *Xenopus* oocytes (Xenopus One, Ann Arbor, MI) were prepared as previously described (MacKinnon, Reinhart, and White, 1988). Oocytes from *Xenopus laevis* were incubated in a saline solution (NaCl, 82.5 mM; KCl, 2.5 mM; $MgCl_2$, 1.0 mM; HEPES, 5 mM; pH 7.6) also containing collagenase (2–4 mg/ml; Gibco-BRL) for 60–90 min and then rinsed thoroughly and stored in an incubating solution (NaCl, 96 mM; KCl, 2 mM; $CaCl_2$, 1.8 mM; $MgCl_2$, 1 mM; HEPES, 5 mM; pH 7.6) containing gentamicin (5 μg/ml). Defolliculated oocytes were selected at least 2 h after collagenase treatment. RNA was injected at least 16 h later. After injection of 5 ng to 50 ng of RNA, oocytes were placed in an incubator at 18°C.

Single-Channel Patch Recording

Tight-seal patch clamp recordings (Axopatch 2B, Axon Instruments, Inc., Foster City, CA) were made 2–4 d after the injection of RNA. Single-channel currents were studied by excising inside-out membrane patches from devitellinized oocytes unless specified otherwise. All recordings were made in the presence of equal concentrations of KCl in the pipette (external) and bath (internal) solutions. The measured signal was filtered at 1 kHz and sampled every 140 μs using an analog to digital converter (Indec Systems, Inc., Sunnyvale, Ca) interfaced with a 386 personal computer. In general, single-channel amplitudes were measured by manually placing cursors at the open and closed channel levels. In some cases, amplitude histograms were constructed from single-channel records. The two methods yielded consistent estimates of single-channel amplitude (see Fig. 2 in Results).

Recording Solutions

Pipette (external) solutions contained KCl (concentrations specified in results), 1 mM $MgCl_2$, 0.3 mM $CaCl_2$ and 10 mM HEPES (pH 7.1). Bath (internal) solutions contained variable concentrations of KCl, 0.5 mM EDTA and 10 mM HEPES (pH 7.1). Oocytes were incubated in bath solution with a desired concentration of K^+, and patches were excised in the same solution. EDTA in the bath solution was used to minimize Ca^{2+}-activated Cl^- current and also to eliminate blockade of ROMK1 channels by internal Mg^{2+}. Fig. 1 *A* shows the effect of 0.5 mM Mg^{2+} on the current produced by many channels in a membrane patch in the presence of 100 mM KCl. The downward curvature of the current trace at positive membrane voltages is due to Mg^{2+} blockade from the inside. When Mg^{2+} was replaced by 0.5 mM EDTA, the *I-V* curve became nearly linear over a range from −80 to 80 mV. The single-channel current recordings made in this study showed the same linearity in the absence of internal Mg^{2+} (Fig. 2).

Channel Run Down

ROMK1 channels gradually disappear (run down) with variable rates after patch excision, and the rate of disappearance becomes faster at higher concentrations of K^+. An example of run down behavior is shown in Fig. 1 *B* where consecutive traces, recorded at 20-s intervals, show a progressive reduction of current. The rapid disappearance of channels made it difficult to record from patches containing only a single channel for any length of time, especially at high K^+ concentrations. We therefore obtained patches containing numerous channels and waited until the number of active channels was small enough to resolve individual transitions. The

traces in Fig. 1 *C* show a patch with a few channels and then finally with only a single channel remaining. Thus, by recording from a patch during the interval when only a few (1–4) channels remain, it was possible to make an accurate measurement of single-channel amplitude.

RESULTS

The Current-Voltage Relationship

Fig. 2 *A* shows a series of representative single-channel current traces recorded in 100 mM KCl solution at voltages between −80 and 80 mV. The mean single-channel

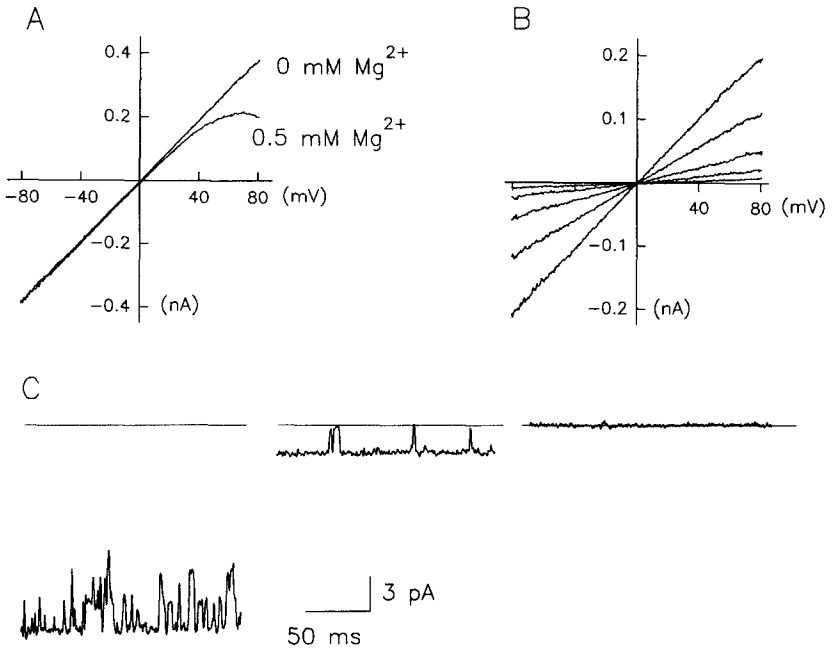

FIGURE 1. Currents were recorded in the presence of 100 mM K^+ on both sides of the membrane. (*A*) Macroscopic currents recorded from a patch containing many (> 100) ROMK1 channels. Membrane voltage was ramped from −80 mV to 80 mV over 1 s. The two traces were recorded from the same patch in the presence of either 0.5 mM Mg^{2+} or 0.5 mM EDTA (0 added Mg^{2+}) in the internal solution. (*B*) Currents were recorded under the same conditions as described in *A* in the absence of internal Mg^{2+} (0.5 mM EDTA). The time between consecutive traces was 20 s; current reduction was due to run down. (*C*) All three traces were obtained from the same patch held at −80 mV. The current trace on the left contains multiple channels. The middle trace was recorded when only a single channel remained active. The trace on the far right was recorded after all channels disappeared. The dished lines identify the close state.

current amplitude from several different patches is plotted as a function of membrane voltage in Fig. 2 *B*. The linear fit on the current-voltage (*i-V*) graph corresponds to a conductance of 30 pS.

The ROMK1 channel has one predominant conducting state but it occasionally enters lower amplitude (subconductance) levels. An example of subconductance behavior is indicated by the arrow below the −80 mV trace in Fig. 2 *A*. The frequency

of such events is relatively rare under the conditions used in this study; the amplitude histogram shown in Fig. 2 *C* shows no appreciable density outside of the closed state and fully conductive open state. All measurements of open-channel current here refer to the predominant conductance state.

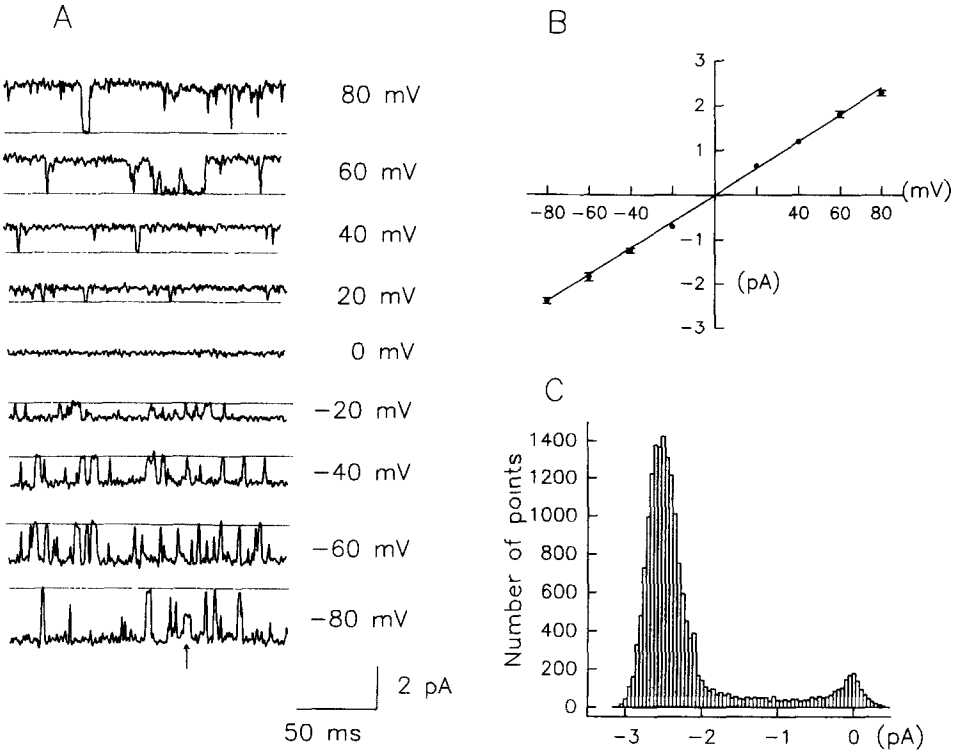

FIGURE 2. The current and voltage relationship of ROMK1. Current was recorded in the presence of 100 mM K^+ on both sides of the membrane. (*A*) Single-channel records show the appearance of unitary openings measured at various potentials. The dashed lines identify the closed state. The arrow underneath the −80 mV current trace indicates a subconducting state. (*B*) Single-channel current amplitude was determined by placing a cursor on the closed and open state levels in records like those in *A*. The current is plotted against the corresponding voltages. Each data point represents the mean ± SEM of measurements made on 5–10 patches. The line corresponds to a conductance of 30 pS. (*C*) An amplitude histogram from a single-channel patch recorded at −80 mV shows that there is a single predominant conducting state.

Conductance as a Function of K^+ Concentration

We next examined the variation of single-channel conductance as K^+ concentration was raised, maintaining equal concentrations on both sides of the membrane. Measurements were made over a range from 10 to 1,000 mM K^+. Fig. 3 *A* shows representative single-channel current traces recorded at −60 mV for each K^+ concentration. Each trace is from a separate patch obtained with equal concentrations of K^+ on both sides of the membrane as indicated. The single-channel current

became larger as K^+ was raised from 10 to 300 mM and then decreased for concentrations above 300 mM. The ragged appearance of the trace recorded in 1,000 mM K^+ is due to patch instability at these concentrations rather than excess open-channel noise.

The *i-V* relationship for ROMK1 was largely linear at all K^+ concentrations studied (Fig. 3, *B* and *C*). For clarity, the *i-V* curves measured between 10 and 300 mM are shown in Fig. 3 *B* and those measured between 300 and 1,000 mM are graphed

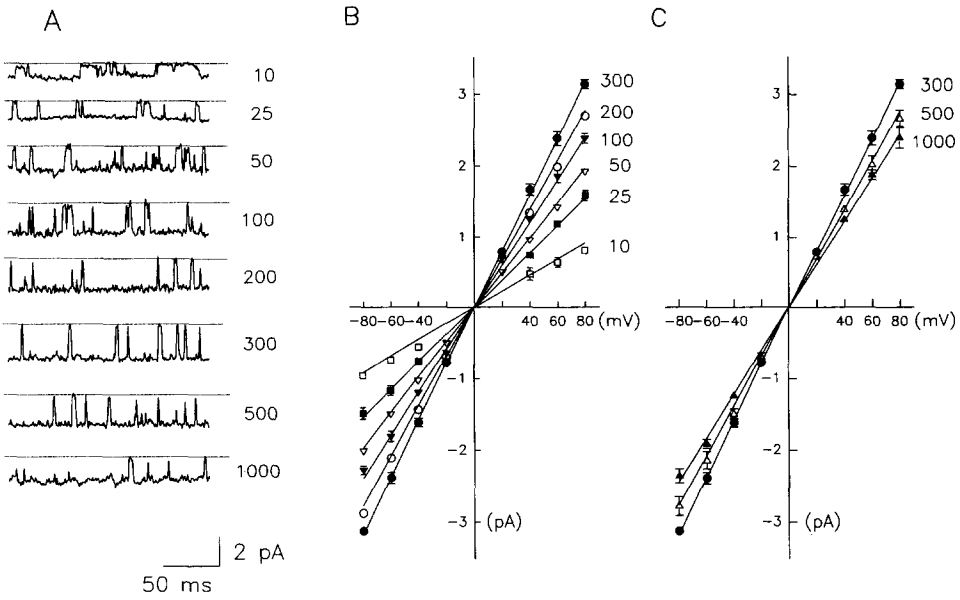

FIGURE 3. The effect of K^+ concentration on the current-voltage relationship. Potassium concentration was varied from 10 to 1,000 mM, maintaining equal concentration on both sides of the membrane. (*A*) Representative single-channel current traces were recorded at various concentrations of K^+ indicated in millimolar. Membrane voltage was −60 mV. The dashed lines identify the closed state. The *i-V* curves, recorded in K^+ concentrations ranging from 10 to 300 mM and from 300 to 1,000 mM, are shown in *B* and *C*, respectively. The number next to each *i-V* curve indicates the K^+ concentration in millimolar. The data points represent the mean ± SEM of single-channel currents measured in at least three patches. The lines superimposed on the data correspond to conductances of 11.5 pS (10 mM), 19.3 pS (25 mM), 24.6 pS (50 mM), 29.9 pS (100 mM), 34.7 pS (200 mM), 39.0 pS (300 mM), 34.5 pS (500 mM) and 30.5 pS (1,000 mM).

separately in Fig. 3 *C*. The slope of the *i-V* relationship, or conductance, increases as K^+ is increased up to 300 mM and then decreases as K^+ is raised further. At 1,000 mM K^+, the conductance is ~75% of its maximum value measured at 300 mM. Fig. 4 shows the conductance plotted as a function of K^+ concentration for the ROMK1 channel (*filled circles*). For comparison, conductance-concentration data from a previously published study on *Shaker* voltage-activated K^+ channels is also included on the graph (Heginbotham and MacKinnon, 1993; *empty circles*).

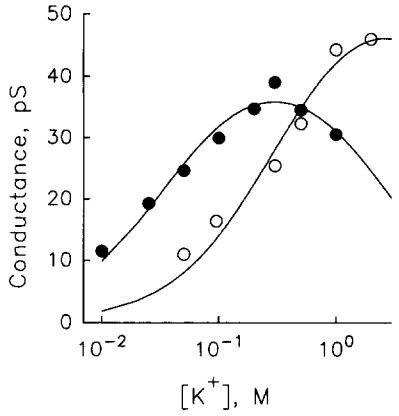

FIGURE 4. The conductance-K^+ concentration relationship. The conductances or *i-V* curve slopes from data shown in Fig. 3 were plotted as a function of the corresponding K^+ concentration (*closed circles*). Similar data previously obtained from a *Shaker* K^+ channel were also plotted as open circles (Heginbotham and MacKinnon, 1993). The curve superimposed on each data set is a least-squares fit using Eq. 1, which yields rate constants $\alpha = 8.1 \cdot 10^8\ M^{-1}\ s^{-1}$, $\beta = 1.0 \cdot 10^9\ s^{-1}$, and $\kappa = 1.4 \cdot 10^7\ s^{-1}$ for the ROMK1 channel, and $\alpha = 1.2 \cdot 10^8\ M^{-1}\ s^{-1}$, $\beta = 1.3 \cdot 10^9\ s^{-1}$, and $\kappa = 1.8 \cdot 10^7\ s^{-1}$ for the *Shaker* K^+ channel.

DISCUSSION

The theoretical basis for a reduction in conductance with increasing ion concentration has been discussed thoroughly in the literature (Hille and Schwarz, 1978; Kohler and Heckmann, 1979; Schumaker and MacKinnon, 1990). The effect is a direct consequence of a conduction mechanism where two or more ions diffuse (or hop from site to adjacent site) along a single-file pathway. In terms of minimal parameter number and analytical tractability, the simplest model case giving rise to such behavior is the single-vacancy pore (Schumaker and MacKinnon, 1990). Fig. 5 shows the state diagram for a single-vacancy pore with two sites. Because the model allows at most only a single vacancy, there are three possible states connected in a triangle. The translocation of an ion through the pore corresponds to a complete cycle around the triangle and conductance is proportional to the change in cycling rate brought about by a change in membrane voltage. As the ion concentration is raised from zero, conductance will increase because ion entry is required to complete a cycle. But when the ion concentration becomes high enough so that the entry rate ($\alpha[X]$) exceeds the internal transition rate (κ), exit from one side will generally be followed by reentry of an ion from the same side. As a consequence, whenever the channel goes from the double occupied state to either one of the single occupied states it will immediately return to the double occupied state along the same path. Thus, sufficiently high ion concentration will reduce the net cycling rate and conductance.

The single-vacancy model is an oversimplification of conduction in a real ion channel, but it is nevertheless instructive to consider the conductance-concentration

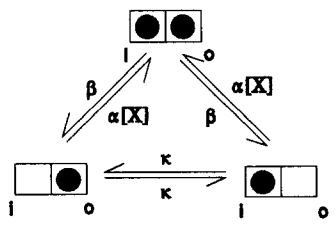

FIGURE 5. A state diagram for a single vacancy model with two K^+ binding sites. The boxes with and without a filled circle represent K^+-occupied and unoccupied states. The rate constants for individual steps are α, β, and κ corresponding to ion entry, exit and internal site-to-site transitions, respectively.

behavior of ROMK1 in terms of the model. For the diagram in Fig. 5, the dependence of zero-voltage conductance on concentration, $[X]$, is given by

$$g = \frac{e^2}{k_B T}\left(\frac{\alpha\kappa\beta[X]}{(\alpha[X] + 2\kappa)(\alpha[X] + 2\beta)}\right) \quad (1)$$

where α, β and κ correspond to ion entry, exit, and internal transition rate constants, respectively (Fig. 5), and e, k_B and T have their usual meanings (Schumaker and MacKinnon, 1990). The curve superimposed on the data for ROMK1 in Fig. 4 corresponds to the fit by Eq. 1 with entry rate constant $\alpha = 8.1 \cdot 10^8\ M^{-1}\ s^{-1}$, exit rate constant $\beta = 1.0 \cdot 10^9\ s^{-1}$, and internal transition rate constant $\kappa = 1.4 \cdot 10^7\ s^{-1}$. (The values for exit and internal transition rate constants may be swapped due to the interchangability of κ and β in Eq. 1.) The simple theory yields a reasonable fit to the ROMK1 conductance-concentration data.

Within the framework of the single-vacancy model, we compared the ROMK1 conductance-concentration data to previously published data obtained for the *Shaker* K^+ channel (Heginbotham and MacKinnon, 1933). The curve in Fig. 4 overlying the values for the *Shaker* channel corresponds to rate constants $\alpha = 1.2 \cdot 10^8\ M^{-1}\ s^{-1}$, $\beta = 1.3 \cdot 10^9\ s^{-1}$, and $\kappa = 1.8 \cdot 10^7\ s^{-1}$. Although a descending phase was not reached experimentally, the data are compatible with a single vacancy conduction mechanism where a maximum conductance would be reached at a concentration of ~2,600 mM. By comparing the rate constants for the two sets of data, we see that an increase in the ion entry rate constant (α) by a factor of 7 can cause the concentration at which the maximum conductance occurs (X_{max}) to decrease from 2,600 to 300 mM. For a two-site single vacancy pore, the dependence of X_{max} on the entry rate can be seen from the relation (Schumaker and MacKinnon, 1990)

$$X_{max} = \sqrt{\frac{4\kappa\beta}{\alpha^2}}. \quad (2)$$

Although X_{max} for the ROMK1 and *Shaker* channels differs by a factor of ~9, the maximal conductance value (g_{max}) is very similar for the two channels. By substituting Eq. 2 into Eq. 1, we see that g_{max} is independent of entry rate constant α and depends only on rate constants κ and β:

$$g_{max} = \frac{e^2}{k_B T}\left(\frac{\kappa\beta}{4\sqrt{\kappa\beta} + 2(\kappa + \beta)}\right). \quad (3)$$

This conclusion can be reached through mere inspection of the diagram in Fig. 5. Because any entry rate ($\alpha[X]$) can be achieved by appropriately adjusting concentration $[X]$, different values of α will shift the location of X_{max} (according to Eq. 2) but g_{max}, the conductance at X_{max}, will not change. These considerations lead us to conclude that the difference in conductance behavior between ROMK1 and *Shaker* K^+ channels may simply be a result of different intrinsic K^+ entry rates. The internal transition and exit rates may be very similar for the two channels.

What at first appears to be a fundamental difference in the conductance behavior of ROMK1 and *Shaker* K^+ channels can be explained by a modest difference in the magnitude of a rate constant. The interpretation given in terms of the single-vacancy

model is entirely consistent with our expectation based on intuition. If ion entry is relatively fast compared to the internal transition and exit rates, then the channel will become saturated at low ion concentrations and a descending phase of the conductance-concentration relationship will be reached. Since ROMK1 and *Shaker* K^+ channels have similar g_{max} values, a change in entry rate alone adequately accounts for the difference in conductance-concentration behavior between these channels.

If a single-vacancy model approximates conduction in K^+ channels in general, then how would high-conductance channels such as Ca^{2+}-activated K^+ channels fit into the description? For these channels, conductance can be greater than 500 pS (Eisenman et al., 1986), i.e., 10 times larger than that of ROMK1 or *Shaker* K^+ channels. Therefore, from Eq. 3, the internal transition and exit rates would have to be considerably faster (by a factor of ~ 10). Suppose that the ion entry rate were the same for ROMK1 and a high-conductance channel. In this case, g_{max} would occur at a much higher concentration in the high-conductance channel (eq 2). By this argument, a lower conductance channel in general (one with a small g_{max}) is more likely to exhibit a conductance maximum at an experimentally achievable ion concentration. Experiments have shown for a high-conductance Ca^{2+}-activated K^+ channel that a conductance maximum is not observed at K^+ concentrations up to 2,000 mM (Eisenman et al., 1986). However, when the experiment is carried out using Rb^+, where g_{max} is lower, a conductance maximum is observed.

In summary, the ROMK1 channel exhibits a conductance maximum at a surprisingly low ion concentration. We have interpreted the results in terms of an oversimplified model of ion conduction in order to consider properties of multi-ion conduction using analytical expressions. Independent of the specific model, the conductance-concentration behavior of ROMK1 reflects an underlying multi-ion conduction mechanism.

We thank K. Ho and S. Hebert for kindly providing the ROMK1 clone and L. Heginbotham for providing data from the *Shaker* K^+ channel for comparison. We also thank A. Gross, L. Heginbotham, P. Hidalgo, and K. Swartz for critically reading the manuscript.

This work was supported by NIH grant GM47400. Z. Lu is a fellow of Harvard Mahoney Neuroscience Institute.

Original version received 18 January 1994 and accepted version received 11 April 1994.

REFERENCES

Armstrong, C. M., R. P. Swenson, and S. R. Taylor. 1982. Block of squid axon K channels by internally and externally applied barium ions. *Journal of General Physiology.* 80:663–682.

Cecchi, X., D. Wolff, O. Alvarez, and R. Latorre. 1987. Mechanisms of Cs^+ blockade in a Ca^{2+}-activated K^+ channel from smooth muscle. *Biophysical Journal.* 52:707–716.

Eisenman, G., R. Latorre, and C. Miller. 1986. Multi-ion conduction in the high-conductance Ca^{2+}-activated K^+ channel from skeletal muscle. *Biophysical Journal.* 50:1025–1034.

Eisenman, G., J. P. Sandblom, and J. L. Walker, Jr. 1967. Membrane structure and ion permeation. *Science.* 155:965–974.

French, R. J., and J. J. Shoukimas. 1985. An ion's view of the potassium channel. The structure of the permeation pathway as sensed by a variety of blocking ions. *Journal of General Physiology.* 85:669–698.

Hagiwara, S., S. Miyazaki, S. Krasne, and S. Ciani. 1977. Anomalous permeabilities of the egg cell membrane of a starfish in K^+-Tl^+ mixtures. *Journal of General Physiology.* 70:269–281.

Heginbotham, L., and R. MacKinnon. 1993. Conduction properties of the cloned *Shaker* K^+ channel. *Biophysical Journal.* 65:2089–2096.

Hille, B., and W. Schwarz. 1978. Potassium channels as multi-ion single-file pores. *Journal of General Physiology.* 72:409–442.

Hladky, S. B., and D. A. Haydon. 1972. Ion transfer across lipid membranes in the presence of gramicidin A. I. Studies of the unit conductance channel. *Biochimica et Biophysica Acta.* 274:294–312.

Ho, K., C. G. Nichols, W. J. Lederer, J. Lytton, P. M. Vassilev, M. V. Kanazirska, and S. C. Hebert. 1993. Cloning and expression of an inwardly rectifying ATP-regulated potassium channel. *Nature.* 362:31–38.

Hodgkin, A. L., and R. D. Keynes. 1955. The potassium permeability of a giant nerve fibre. *Journal of Physiology.* 128:61–88.

Kohler, H. H., and K. Heckmann. 1979. Unidirectional fluxes in saturated single file pores of biological and artificial membranes I. Pores containing no more than one vacancy. *Journal of Theoretical Biology.* 79:381–401.

MacKinnon, R., P. H. Reinhart, and M. M. White. 1988. Charybdotoxin block of *Shaker* K^+ channels suggests that different types of K^+ channels share common structural features. *Neuron.* 1:997–1001.

Neyton, J., and C. Miller. 1988. Potassium blocks barium permeation through calcium-activated potassium channels. *Journal of General Physiology.* 92:549–567.

Schumaker, M. F., and R. MacKinnon. 1990. A simple model for multi-ion permeation. Single-vacancy conduction in a simple pore model. *Biophysical Journal.* 58:975–984.

Shapiro, M. S., and T. E. DeCoursey. 1991. Selectivity and gating of the Type *L* Potassium channel in mouse Lymphocytes. *Journal of General Physiology.* 97:1227–1250.

Villarroel, A., O. Alvarez, and G. Eisenman. 1988. A maximum in conductance occurs for the large Ca^{2+}-activated K^+ channel at high Rb^+ concentration. *Biophysical Journal.* 53:259*a*. (Abstr.)

Wagoner, P. K., and G. S. Oxford. 1987. Cation permeation through the voltage-dependent potassium channel in the squid axon. Characteristics and mechanisms. *Journal of General Physiology.* 90:261–290.

Yellen, G. 1984. Ionic permeation and blockade in Ca^{2+}-activated K^+ channels of bovine chromaffin cells. *Journal of General Physiology.* 84:157–186.